Regioselectivity of Meisenheimer complexation in reaction of oxygen-centred nucleophiles with picryl aryl ethers: Polar vs. SET mechanisms

Erwin Buncel, Julian M. Dust, Richard A. Manderville, and Richard M. Tarkka

Abstract: Picryl alkyl ethers react with hydroxide and methoxide ions to give regioisomeric Meisenheimer (anionic σ-) adducts; the C-3 adduct is kinetically favoured and the C-1 adduct is thermodynamically favoured (K3T1 behaviour). In the current 400 MHz NMR spectroscopic study of the reactions of two picryl aryl ethers, picryl phenyl ether (PicOPh, **1**) and picryl mesityl ether (PicOMes, **2**), the charge localized nucleophiles OH^- and MeO^- displayed the same K3 regioselectivity as found with picryl alkyl ethers; attachment at C-1 leads to S_NAr displacement of the aryloxide. In contrast, phenoxide (PhO^-) and the sterically demanding 2,4,6-trimethylphenoxide (mesitoxide, $MesO^-$) react with **1** and **2** to form the C-1 O-adduct as the product of kinetic control (i.e., K1 behaviour). These reactions were studied at low temperature (–40°C in acetonitrile-d_3:dimethoxyethane-d_{10} 1:1) and as a function of increasing temperature (–40°C to ambient). On the thermodynamic side, the C-1 PhO^- O-adduct of **1** is also the more stable of the possible phenoxide O-adducts; it shows T1 regioselectivity within the manifold of O-adducts (K1T1), but the C-3 C-adduct (via *para*-attack of PhO^-) is the ultimate thermodynamic product. The C-1 O-adducts formed by $MesO^-$ with **1** or **2** give way with time (or temperature increase) in favour of their C-3 regioisomers or a C-1,3-O-diadduct. Mesitoxide, therefore, displays K1T3 regioselectivity. Stereoelectronic stabilization is discussed as a factor influencing T1 regioselectivity in O-adduct formation. Frontier molecular orbital (FMO) interactions between the HOMO of the nucleophile and the LUMO of the picryl ether may play a role in the K1 preference of aryloxides. An alternative argument is presented based on a single electron (radical) transfer (SET) pathway for the aryloxide nucleophiles rather than the polar (S_NAr) pathway for hydroxide and methoxide. The SET pathway also predicts a kinetic preference for C-1, as the C-1 position is of higher spin density than C-3 in the radical anion of the picryl ether and thus should be the preferred site for coupling by the aryloxide radical.

Key words: anionic Meisenheimer adducts, regioselectivity, kinetic–thermodynamic control, FMO, stereoelectronic stabilization, single electron transfer (SET).

Résumé : Les oxydes de picryle et d'alkyle réagissent avec les ions hydroxydes et méthylates avec formation d'adduits (anioniques σ-) de Meisenheimer régioisomères; l'adduit en C-3 est favorisé d'un point de vue cinétique alors que l'adduit en C-1 est favorisé d'un point de vue thermodynamique (comportement K3T1). Dans l'étude courante, par spectroscopie RMN à 400 MHz, des réactions de deux oxydes de picryles et d'aryles, l'oxyde de picryle et de phényle (PicOPh, **1**) et l'oxyde de picryle et de mésityle (PicOMes, **2**), les nucléophiles à charge localisée, OH^- et MeO^-, présentent la même régiosélectivité K3 que celle observée avec les oxydes de picryle et d'alkyle; la fixation en C-1 conduit à un déplacement S_NAr de l'aryloxyde. Par opposition, le phénolate (PhO^-) et le 2,4,6-triméthylphénolate (mésitylate, $MesO^-$) qui imposent des demandes stériques beaucoup plus importantes réagissent tous les deux avec les composés **1** et **2** pour former, comme produit de contrôle cinétique, un O-adduit en C-1 (comportement K1). On a étudié ces réactions à basse température (–40 °C, dans un mélange acétonitrile-d_3:diméthoxyéthane-d_{10} 1:1) et en fonction d'une augmentation de la température (–40 °C à la température ambiante). D'un point de vue thermodynamique, le O-adduit du PhO^- en C-1 du produit **1** est aussi le plus stable des O-adduits possibles pour le phénolate; il présente du régiosélectivé T1 parmi les plusieurs O-adduits (K1T1); toutefois, le C-adduit C-3 (obtenu par une attaque en *para* du

Received 5 November 2002. Published on the NRC Research Press Web site at http://canjchem.nrc.ca on 17 April 2003.

Dedicated to Prof. Don Arnold for his contributions to chemistry in Canada.

E. Buncel.[1] Department of Chemistry, Queen's University, Kingston, ON K7L 3N6, Canada
J.M. Dust.[2] Departments of Chemistry and Environmental Science, Sir Wilfred Grenfell College, Corner Brook, NL A2H 6P9, Canada.
R.A. Manderville.[3] Department of Chemistry, Wake Forest University, Winston-Salem, NC 27109-7486, U.S.A.
R.M. Tarkka. Department of Chemistry, University of Central Arkansas, Conway, AR 72035, U.S.A.

[1]Corresponding author (e-mail: buncele@chem.queensu.ca).
[2]Corresponding author (e-mail: jdust@swgc.mun.ca).
[3]Corresponding author (e-mail: manderra@wfu.edu).

 doi: 10.1139/V03-014

PhO^-) est le produit thermodynamique ultime. Les O-adduits C-1 qui se forment initialement entre le $MeSO^-$ et les produits **1** et **2** laissent la place, avec le temps ou une augmentation de la température, à leurs régioisomères C-3 ou à un C-1,3-O-diadduit. Le mésitylate présente donc une régiosélectivité K1T3. On discute de la stabilisation électronique comme facteur influençant la régiosélectivité T1 dans la formation des O-adduits. Les interactions des orbitales moléculaires frontières (OMF) entre l'OM haute occupée et la basse vacante de l'oxyde de picryle pourrait jouer un rôle dans la préférence K1 des aryloxydes. On présente un argument alternatif, basé sur une voie réactionnelle impliquant le transfert d'un seul (radical) électron (SET) pour les nucléophiles aryloxydes plutôt qu'une voie polaire (S_NAr) pour l'hydroxyde et le méthanolate. La voie SET permet aussi de prédire une préférence cinétique pour C-1 parce que cette position possède une densité de spin plus élevée que celle en C-3 dans l'anion radical de l'oxyde de picryle et qu'elle devrait donc être le site favorisé pour le couplage avec le radical aryloxyde.

Mots clés : adduits anioniques de Meisenheimer, régiosélectivité, contrôles cinétique et thermodynamique, OMF, stabilisation stéréoélectronique, transfert d'un seul électron (SET).

[Traduit par la Rédaction]

Introduction

Reaction of a base (nucleophile) with an electron-deficient aromatic may give rise to diverse products, namely π-complexes (1), radical anions (2), aryl carbanions (3), and anionic σ-adducts (termed Meisenheimer complexes) (1–4). With 1-X-2,4,6-trinitrobenzenes, nucleophiles react to form Meisenheimer complexes according to an accepted general pattern of the initial formation of a C-3 adduct that gives way over time to a thermodynamically favoured C-1 adduct (5). This regioselectivity has been elaborated in a number of 1-X-2,4,6-trinitrobenzene-nucleophile reaction systems, notably with alkoxides and hydroxide as nucleophiles (5), and has been labelled K3T1 (6, 7) (cf. Fig. 1).

In a series of articles (6, 7), we have delineated a full range of regioselectivities in Meisenheimer complexation. Thus, while 2,4,6-trinitroanisole (TNA) reacts with methoxide according to the K3T1 pattern (cf. Fig. 1) (5*a–d*, 6*b*), TNA reacts with the oxygen centre of a phenoxide ion (PhO^-) with K1T1 regioselectivity. In the latter case, a C-1 TNA·OPh^- adduct was the first (and only) phenoxide O-adduct detected by 400 MHz ^{1}H NMR spectroscopy at –40°C in acetonitrile–dimethoxyethane (MeCN-d_3:DME-d_{10} 1:1) solvent (6*b*). The regioisomeric C-3 TNA·OPh^- adduct was not observed, in accord with a previous stopped-flow UV–vis kinetic study in which the initially observed adduct was identified as the C-1 species (8). Furthermore, the structurally similar phenoxide O-adduct of 1,3,5-trinitrobenzene (i.e., TNB·OPh^-) can be observed by ^{1}H NMR spectroscopy under the same conditions used in the TNA·PhO^- study (9*a*). On this basis, the regioselectivity exhibited by the TNA–PhO^- system was classified as K1T1, i.e., a system in which the C-1 adduct is favoured by both kinetics and thermodynamics (Fig. 1). However, the ultimate phenoxide product was the C-3 TNA·$PhO(H)^-$ *para* C-bonded adduct, consistent with the ambident (O- and C-) nucleophilic nature of PhO^- (6*b*) and in agreement with results gleaned from related systems (9). The behaviour of phenoxide as a C-nucleophile corresponds to K3T3 regioselectivity wherein the C-3 C-adduct is the product of both kinetic and thermodynamic control. Our AM1 calculations on the regioisomeric adducts formed by TNA with OH^- and CH_3^- as prototypical O- and C-nucleophiles, respectively, confirm the thermodynamic preference for C-3 attack by carbon nucleophiles (6*d*). This K3T3 behaviour (Fig. 1) of C-nucleophiles is also implicit in the synthetic results found in vicarious nucleophilic substitution (VNS) reactions, as documented by Makosza and co-workers (10). Finally, we have reported the results of the reaction of TNA with the bulky aryloxide nucleophile 2,4,6-trimethylphenoxide (mesitoxide, $MesO^-$) (6*c*). In this system, attack at C-1 to yield a C-1 TNA·$OMes^-$ Meisenheimer complex is kinetically favoured at –40°C, but as the NMR probe temperature was raised, the C-1 adduct rapidly declined in concentration and was supplanted by the C-3 TNA·$OMes^-$ adduct, in accord with K1T3 behaviour (Fig. 1). This reactivity pattern is the inverse of the "normal" K3T1 isomerization pathway displayed by alkoxides and hydroxide.

Although a wide range of kinetic and thermodynamic factors have been advanced (4, 5, 11, 12) to account for the regioselectivity found in picryl ether – base Meisenheimer complexation, our analysis has focused primarily on thermodynamics and has highlighted the contribution made by stereoelectronic stabilization of the relevant C-1 adducts (6*b–d*, 7, 9*a*). In this approach, C-1 adducts, as acetal analogues, can be stabilized by $n \rightarrow \sigma^*$ donation from an oxygen lone pair of one RO group into the anti-bonding orbital of the C—OR bond (and vice versa); the interaction is maximized if the relevant lone pairs and C—OR fragment bonds can be arranged antiperiplanar to one another. Where stereoelectronic stabilization is negligible, the C-3 adduct may become the thermodynamic product (7).

The arguments concerning kinetic factors have either relied on assumptions made about the position of the transition state for adduct formation (5*d*, 6*b*) or have consisted of assessments of steric hindrance to attack at C-1 (F-strain) (11, 12*d*, 12*e*, 13, 14). In light of the K1T3 behaviour exhibited in the reaction of TNA with mesitoxide, a bulky nucleophile, the importance of F-strain in determining the regioselectivity of Meisenheimer complexation warrants re-examination.

The present article extends the study of picryl ether – nucleophile interactions to the picryl *aryl* ethers picryl phenyl ether (PicOPh, **1**) and picryl mesityl ether (PicOMes, **2**). The reactions of these ethers, **1** and **2**, with the aryloxide nucleophiles, phenoxide ion (PhO^-) and mesitoxide ($MesO^-$), were monitored in acetonitrile–dimethoxyethane (MeCN-d_3:DME-d_{10} 1:1 v/v) as a function of temperature (–40° to ambient), and the PicOPh–PhO^- system was studied in dimethyl sulfoxide (DMSO-d_6) at room temperature. Thus, the current study

Fig. 1. Qualitative comparative energy-reaction coordinate profiles for the four general patterns of regioselectivity. Barrier heights and relative stabilities are exaggerated for clarity. K3T1 describes those systems in which formation of the C-3 adduct is the product of *kinetic* control, but the C-1 adduct is the *thermodynamic* product. In the K1T1 profile the C-1 adduct is favoured by both kinetics and thermodynamics. The profile designated K3T3 represents the situation where the C-3 adduct is doubly preferred; that is by kinetics and by thermodynamics. The K1T3 profile describes the inverse behaviour from that indicated by K3T1; now the C-1 adduct is favoured kinetically but the C-3 adduct is the most stable product.

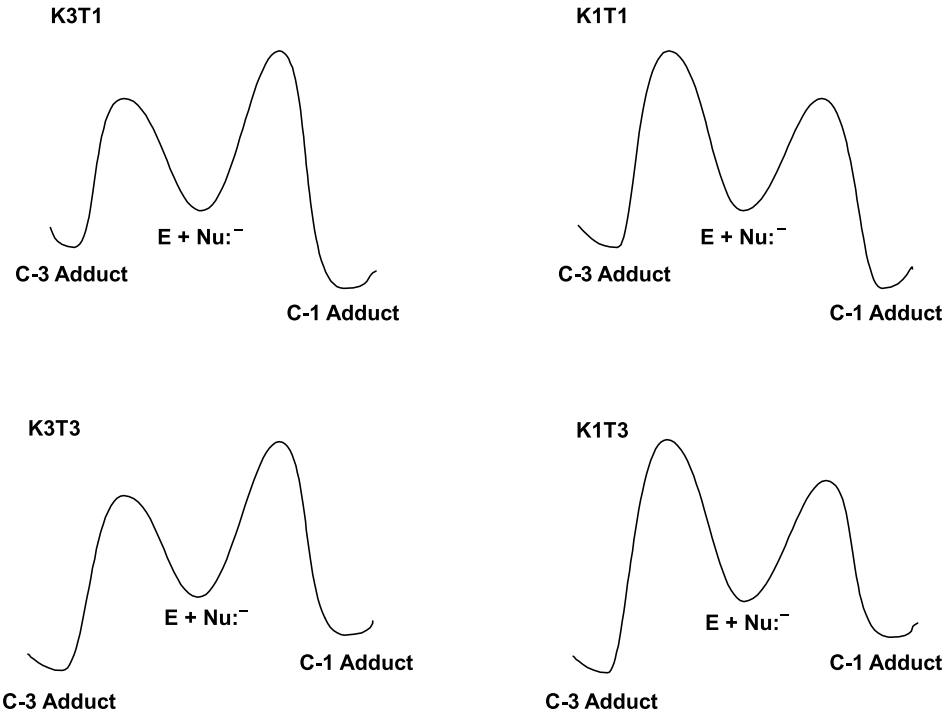

further probes the effect of steric hindrance at C-1 on the kinetics of these systems, particularly in the case of the highly hindered PicOMes reacting with the bulky $MesO^-$ anion.

The results are compared with those obtained in the related TNA–Nu^- systems and are discussed with regard to possible frontier molecular orbital (FMO) interactions between the highest occupied molecular orbital (HOMO) of the aryloxide nucleophiles and the lowest unoccupied molecular orbital (LUMO) of the polynitroaromatic substrate. To model a 1-X-2,4,6-trinitrobenzene, we have carried out a semi-empirical (AM1) (15) molecular orbital calculation on TNA, and these results are included in this article. Finally, more recent suggestions that related reactions proceed through transition states having varying degrees of radical character (16) or via single electron transfer (SET) to give a radical–radical anion pair (2) are considered.

Results

Reactions of the aryloxides PhO^- and $MesO^-$ with the electrophiles PicOPh, **1**, and PicOMes **2**, were monitored by 400 MHz ^{1}H NMR in acetonitrile–dimethoxyethane (MeCN-d_3-DME-d_{10} 1:1 v/v), a solvent system that has proven useful in NMR studies down to temperatures of –50°C (6*b*, 6*c*, 9*a*). Reactions of **1** and **2** with OH^- and MeO^- were conducted in DMSO-d_6 at ambient temperature. Spectroscopic characteristics of the species (including coupling constants, *J*, in Hz) shown in Schemes 1 and 2 are listed in Table 1. In general, resonances are located at positions farther downfield in the MeCN-d_3:DME-d_{10} medium than in DMSO-d_6. ^{13}C NMR peak positions for some relevant σ-adducts measured in MeCN–DME and substrates measured in DMSO-d_6 are given in Table 2.

As in previous studies of the reaction of aryloxides with picryl systems (6*b*, 6*c*, 9), C-3 hydroxide adducts of **1** (i.e., **6**) and **2** (i.e., **15**) were observed also. The assignment of the signals of these adducts (**6** and **15**) was confirmed by control experiments that involved the electron-deficient substrates and tetramethylammonium hydroxide (Me_4NOH) in DMSO. In general, these C-3 hydroxide adducts gave way over time to picrate anion ($PicO^-$, **8**) following a pattern seen previously (6*b*, 6*c*, 9). Methoxide reacted with **1** and **2** to yield the respective C-3 adducts **9** and **17**, as the products of kinetic control; the corresponding C-1 adducts **10** and **18** were not observed. Relevant spectroscopic data for the observed adducts are given in Table 1.

Reaction of 1 with excess PhOK in MeCN–DME

To an NMR tube that contained a solution of PicOPh (**1**) in MeCN-d_3:DME-d_{10} (1:1, v/v), cooled to –50°C, was injected 1.5 equiv of a similarly cooled MeCN-d_3:DME-d_{10} solution of phenoxide ion (PhOK; final concentrations of **1**:PhOK were 0.06:0.09 M). The first ^{1}H NMR spectrum recorded at –40°C contained a singlet at δ 8.63 that is consistent with the resonance for two equivalent ring protons ($H_{3,5}$) of a C-1 O-adduct. Other signals in the spectrum are similarly attributable to the C-1 PicOPh·OPh^- O-adduct, **3** (Scheme 1). The initial low-temperature spectrum was re-

Scheme 1.

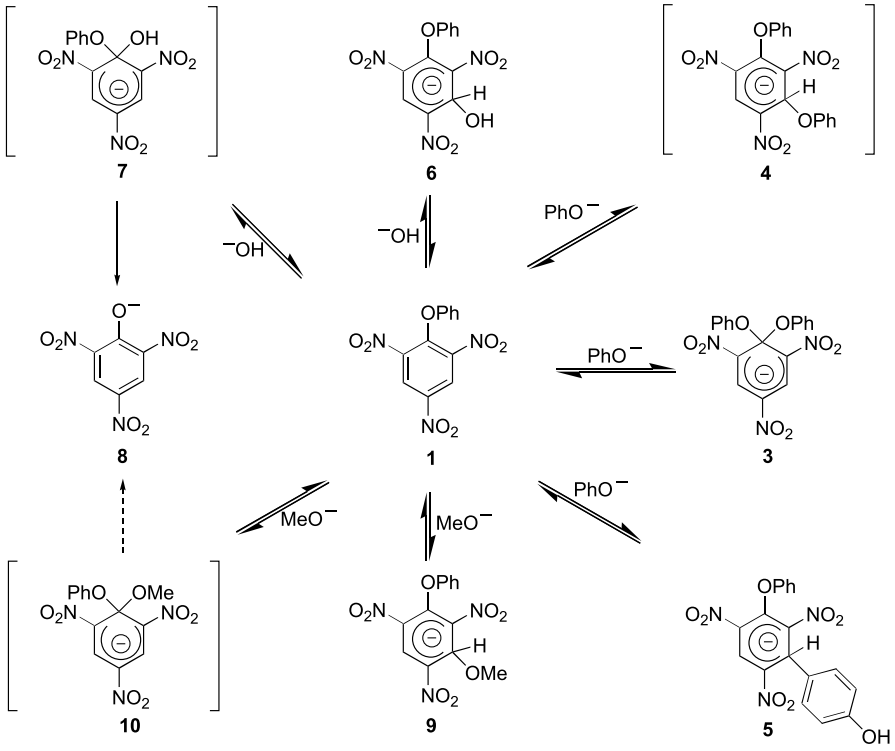

markably free from signals that would arise from formation of other adducts at this temperature. Therefore, a full assignment could be made for **3**: 8.63 (2H, s, $H_{3,5}$), 7.15 (4H, m, H_m), 6.95 (2H, m, H_p), and 6.69 (2H, m, H_o).[4] It is pertinent to note that the signals assigned to the ring protons of the attached phenoxyl group are equivalent, indicating that the adduct is symmetrical. The ^{13}C NMR spectrum of **3** was also recorded (Table 2).

As the temperature was gradually raised, resonances of **3** began to broaden, and after ca. 1 h at 10°C a new set of doublets could be seen at 8.57 (1H, J = 1.9) and 6.42 (1H, J = 1.9). These peaks are assignable to H_5 and H_3, respectively, of the C-3 PicOPh·OH$^-$ adduct, **6** (Scheme 1), that arises from equilibration of PhO$^-$ and adventitious water present in the solvent (cf. ref. 6b, 6*c*, 17). The OH resonance of **6** was not observed and its state of ionization is, therefore, uncertain.

As the temperature was further raised to ambient, a singlet was noted at 8.65. Comparison with related systems (6) shows that this singlet represents the two equivalent ring protons of picrate anion, i.e., PicO$^-$, **8**. Eventually (>5 h) peaks appear that are ascribable to the C-3 *para*-bonded adduct, **5** (Scheme 1); resonances belonging to **5** are given in Table 1. The OH of the attached phenoxyl group was not observed, so the state of ionization of this OH is uncertain. Moreover, the *para* proton (H_p) of the C-1 phenoxyl moiety of the C-3 PicOPh·PhO(H)$^-$ adduct, **5**, was apparently obscured by resonances of free PhOH (i.e., $H_{m'}$, $H_{o'}$, $H_{p'}$).

In summary, as an O-nucleophile, PhO$^-$ reacts at C-1 of PicOPh, **1**, to yield the C-1 O-adduct, **3**, as the first phenoxide adduct. More significantly, at no time were peaks observed that could be attributed to a C-3 phenoxide O-adduct (i.e., **4**, Scheme 1). We have previously shown (9*a*) that the chemical shift of the diagnostic proton bonded to the sp^3-hybridized ring carbon in the phenoxide O-adduct of 1,3,5-trinitrobenzene, TNB·OPh$^-$, is located 0.5–0.8 ppm downfield from the signal for the comparable proton in analogous TNB·OR$^-$ adducts. On this basis, the signal for the similar sp^3-bound proton in the putative C-3 PicOPh·OPh$^-$ adduct, **4**, should appear in a region of the spectrum well separated from the signals of the C-3 hydroxide adduct, **6**, and so should be readily identifiable. In fact, no such signal was seen before the appearance of the peaks assigned to the C-1 O-adduct, **3**, nor did it appear later in response to increasing temperature. As the temperature was raised, **6** and PicO$^-$, **8**, were observed in the spectrum. Slowly, **6** gave way to **8** and free phenol, presumably through the intermediacy of a transient C-1 PicOPh·OH$^-$ adduct, **7**, that is not observed. Such adducts have been postulated in analogous reaction systems (6*b*–*d*). In accord with the ambident nature of phenoxide ion, the eventual product of phenoxide attack is the C-3 *para* C-bonded adduct, **5**.

Reaction of 1 with equimolar MesOK in MeCN–DME

Upon addition of 1 equiv of potassium 2,4,6-trimethylphenoxide ion (potassium mesitoxide, MesOK) in MeCN-d_3:DME-d_{10} to the NMR tube that contained a cooled (–50°C) solution of **1** (final concentration 0.06 M), the sample turned a deep orange colour. Interestingly, the initial ^{1}H NMR spec-

[4] Signals assigned to the *para*, *meta*, and *ortho* (H_p, H_m, and H_o) protons typically appear as somewhat broadened triplets, and triplets and doublets, respectively. The broadening found is indicative of further unresolved coupling and so throughout this article the signals ascribed to attached phenoxyl groups and to phenoxide ion or phenol will be listed as multiplets.

Scheme 2.

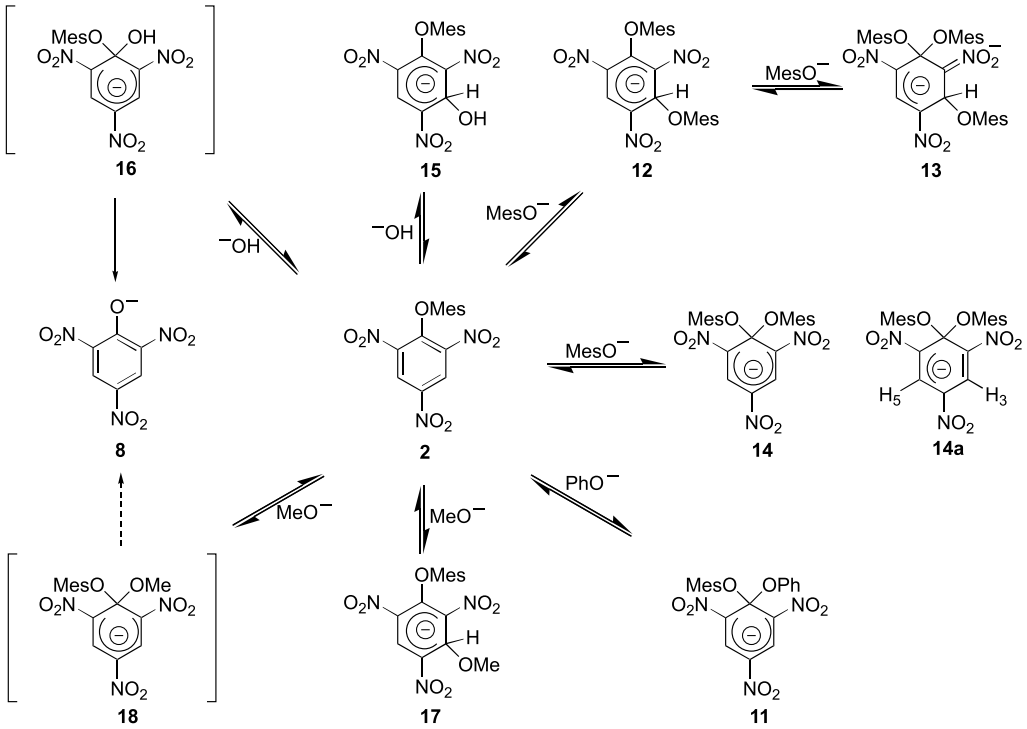

trum, recorded at –40°C, showed the presence of *two* σ-complexes, the C-1 PicOPh·OMes⁻ O-adduct, **11** (Scheme 2), and the C-1 PicOPh·OPh⁻ adduct, **3** (Scheme 1). At this stage, peaks of **11** were found at δ 8.69 (2H, s, $H_{3,5}$), 7.08 (2H, m, H_m), 6.80 (1H, m, H_p), 6.68 (2H, s, $H_{3',5'}$ mesitoxyl), 6.60 (2H, m, H_o), 2.16 (3H, s, *p*-Me, mesitoxyl), and 1.97 (6H, s, *o*-Me) and were clearly distinguishable from the signals assigned to **3** (Table 1). The resonances of **11** were predominant in this initial spectrum: **11**:**3** = 2:1.

As the temperature of the system was slowly raised to −20°C, broad resonances appeared, a set at ca. 8.60 and 6.80 and a signal at ca. 6.67; these resonances were ascribable to PicOMes, **2**, and mesitol (MesOH), respectively. Coincident with the appearance of the new signals, the resonances assigned to **11** declined in favour of those of **3.** With the increase to –10°C and the passage of time (ca. 2 h), new resonances appeared that were assigned to C-3 aryloxide O-adducts. The sp^3-bound protons (H_3) of the O-adducts were doublets at 6.90 (J = 2.2) and 6.87 (J = 2.2), whereas the sp^2-bound protons (H_5) appeared as a single triplet that arises from overlapping doublets centred at 8.43. The downfield shift of the H_3 protons (at 6.90 and 6.87) of these species relative to the shift of the corresponding proton established for the C-3 PicOPh·OH⁻ adduct, **6**, was consistent with attachment of the O-centre of an aryloxide (6, 9*a*). Although additional signals that would be expected for these C-3 aryloxide O-adducts were obscured by the peaks of **2**, **3**, **11**, and MesOH, the signals at 6.90, 6.87, and 8.43 (as well as those for **3**, **6,** and **11**) do not survive acidification (trifluoroacetic acid, TFA; 5 μL); it is a characteristic of O-adducts that they are acid labile (4*b*, 6, 9). Tentative assignment of the structures of the C-3 O-adducts corresponding to the 6.90, 6.87, and 8.43 set of signals will be made below.

Subsequent monitoring of the reaction as a function of increasing temperature (from –10 to 0°C in ca. 30 min) showed that the peaks due to **11** vanished while signals attributed to **3** and the C-3 aryloxide O-adducts remained in the spectrum. Furthermore, peaks assigned to the PicOPh·OH⁻ adduct, **6**, were joined by those of the C-3 PicOMes·OH⁻ adduct, **15** (Table 1, Scheme 2). At ambient temperature the signals attributed to **3** and the C-3 aryloxide O-adducts were no longer present; those of the OH⁻ adducts, **6** and **11**, dominated the spectrum. Peaks for **2**, MesOH, and **8** were also found and a spectrum acquired after 2 days at ambient still contained peaks for **8** and mesitol as well as PhOH.

Thus, the results suggest that in the reaction of MesO⁻ with **1,** initial attack gives the C-1 PicOPh·OMes⁻ O-adduct, **11**. Breakdown of **11** via an S_NAr pathway (18–20) leads to formation of PicOMes and PhO⁻ and, therefore, to a system that contains two substrates (**1** and **2**) as well as two nucleophiles (PhO⁻ and MesO⁻). The liberated PhO⁻ ion reacts at C-1 of **1** to give **3**. As the reaction proceeds, peaks due to **11** decrease in intensity in tandem with growth of the resonances of **2**, MesOH and **3**. At no time are peaks of **1** and free PhOH observed at this early stage of the reaction.

The next observable σ-adducts appeared at –10°C and were identifiable as C-3 aryloxide O-adducts (6, 9*a*). Although the exact assignment of these adducts is tentative, the spectroscopic evidence supports the assignment of the signals to C-3-type aryloxide O-adducts. Moreoever, the C-3 adducts arise from attack of MesO⁻ on **2** and are not C-3 adducts formed by attack of either PhO⁻ or MesO⁻ on **1**. First, the previous experiment (vide supra) confirmed PhO⁻ attack at C-1 of **1** to give **3** as the only process that involves **1** and phenoxide as an O-nucleophile. Thus, none of the C-3 arylo-

Table 1. ^{1}H NMR spectroscopic characteristics[a] of the C-1 and C-3 adducts formed by PicOPh, **1**, and PicOMes, **2**, with phenoxide, mesitoxide, hydroxide, and methoxide ions.

Adduct	H-5	H-3	Other signals	Adduct	H-5	H-3	Other signals
3[b,c]	8.63, s	8.63, s	7.15 (m, Hm), 6.95 (m, Hp), 6.69 (m, Ho)	**12**[b,c]	8.44, d J = 2.0	6.90, d J = 2.0	Obscured
5[b,d]	8.57, d J = 1.2	5.77, d J = 1.2	7.08, 6.64 (A2X2, J = 8.5), 7.21 (m, C-1 Hm), 6.90 (m, C-1 Hp)	**13**[b,c]	8.44, d J = 2.0	6.87, d J = 2.0	Obscured
6[e,f]	8.47, d J = 1.9	6.30, d J = 1.9	7.27 (m, Hm), 6.98 (m, Hp), 6.91 (m, Ho)	**14**[b,f]	8.63 br s	7.17 br s	6.50–6.80 (mesitoxyl), 1.9–2.2 (s, *o*-,*p*-Me)
9[e,f]	8.56, d J = 1.9	6.24, d J = 1.9	7.28 (m, Hm), 6.99 (m, Hp), 3.27 (s, C-3 OMe)	**15**[e,f]	8.39 br s	6.13 br s	6.73, 6.71 (s, C-1 mesitoxyl), 2.16, 2.12, 1.96 (s, *o*-,*p*-Me)
11[b,d]	8.69, s	8.69, s	7.08 (m, Hm), 6.80 (m, Hp), 6.68 (s, mesitoxyl ring), 6.60 (m, Ho), 2.16 (s, *p*-Me), 1.97 (s, *o*-Me)	**17**[e,f]	8.43, d J = 2.0	5.99, J = 2.0	6.76, 6.73 (s, C-1 mesitoxyl), 2.18, 2.16, 2.03 (s, *o*-,*p*-Me)

[a]Chemical shifts were measured in ppm (δ) at 400.1 MHz; coupling constants are reported in Hz.
[b]MeCN-d_3:DME-d_{10} (1:1, v/v).
[c]Recorded at –40°C.
[d]Recorded at 0°C.
[e]Recorded at room temperature.
[f]DMSO-d_6.

xide O-adducts can arise from interaction of **1** and PhO^-. Secondly, decomposition of the initially formed C-1 PicOPh·OMes$^-$ adduct, **11**, releases PicOMes, **2**, which could undergo further attack by mesitoxide. Note that **2** and MesOH are both observed in spectra acquired at this temperature. Further justification for the assignments was obtained from study of the PicOMes–$MesO^-$ system (vide infra). By the reasoning outlined, the peaks of the C-3 aryloxide O-adducts in the present system are ascribed to the C-3 PicOMes·OMes$^-$ adduct, **12**, and the C-1,3 PicOMes·$(OMes)_2^{2-}$ diadduct, **13**. The H_3 resonance at 6.90 (d, J = 2.2) is attributed to **12**; that of **13** appears at 6.87 (d, J = 2.2).

The final σ-adducts found in the system are the C-3 hydroxide complexes **6** and **15** that result from equilibration of PhO^- and $MesO^-$ with residual water in the medium that, in turn, generates OH^-. Ultimately, these too give way to picrate ion, **8**, PhOH, and MesOH.

Reaction of 2 with equimolar PhOK in MeCN–DME

The interaction of PicOMes, **2**, with PhOK in MeCN-d_3:DME-d_{10} (1:1 v/v) was found to give results similar to those for the PicOPh–$MesO^-$ reaction system described above. Consequently, after the addition of equimolar PhOK in MeCN-d_3:DME-d_{10} to a solution of **2** in the same medium (final concentrations: 0.06 M), cooled to –50°C, the first spectrum (recorded at –40°C) includes resonances of the C-1 PicOMes·OPh^- O-adduct, **11** (Scheme 2) as well as the C-1 PicOPh·OPh^- O-adduct, **3** (Scheme 1). As the temperature is raised, peaks reappear for **2** and appear for MesOH, but at –10°C, signals are observed that correspond to the C-3 mesitoxide adducts, **12** and **13**. Observation of the peaks for these species validates their observation and assignment in the PicOPh–$MesO^-$ reaction system.

Peaks due to **11** disappear from the spectrum at 0°C and resonances attributable to the C-3 hydroxide adducts, **6** and **15**, appear. At ambient temperature the signals for these hydroxide adducts, **6** and **15**, and for $PicO^-$ were dominant, whereas the peaks of **3**, **12**, and **13** diminish. Eventually (>12 h), the spectrum obtained at room temperature consists mainly of **8**, PhOH, and MesOH, although small extraneous, unidentified signals were also present.

Reaction of 2 with equimolar MesOK in MeCN–DME

To a solution of **2**, cooled to –50°C, was added a similarly cooled solution of MesOK in MeCN-d_3:DME-d_{10} (final concentration: 0.06 M). The major peaks in the initial ^{1}H NMR spectrum measured at –40°C (acquired within 5 min of mixing) were identified as belonging to unmodified **2** and MesOK. However, two equivalent broad singlets were also noted at δ 8.62 and 7.17. The 8.62 resonance could correspond to the $H_{3,5}$ protons of a C-1 $MesO^-$ adduct; comparison of the chemical shift with those for the $H_{3,5}$ protons of the related C-1 TNA·OMes$^-$ adduct, **18**, (i.e., 8.62 (6*c*)) and the C-1 PicOPh·OPh^- adduct, **3** (i.e., 8.63) favours this assignment. However, in the present system the relative integrals link the 8.62 peak to the broad signal at 7.17 (i.e., 1:1 integral ratio). Moreover, peaks, albeit poorly resolved ones, are observed in the 6.5–6.8 and 1.9–2.2 ppm regions (other than those for **2** and MesOK) and are taken to represent the mesitoxyl protons of this initially formed species.

Table 2. ^{13}C NMR spectral characteristics[a] of the C-1 PicOPh phenoxide adduct, **3**, and the C-1 TNA phenoxide adduct **10**,[b] in MeCN–glyme,[c] as well as the substrates, PicOMe (TNA), PicOPh (**1**), and PicOMes (**2**) in DMSO.[d]

Species	C-1	C-2,6	C-3,5	C-4	C-7	C-8,12	C-9,11	C-10
3[c]	104.4	130.8	130.5	119.9	155.1	120.8	130.4	124.0
10[b,c]	104.5	129.5	131.1	119.7	155.4	120.5	130.4	124.0
TNA[d]	151.5	144.3	125.0	141.7	65.2			
1[d]	145.2	144.0	125.5	143.3	156.4	115.8	130.1	124.6
2[d,e]	145.5	141.0	124.4	140.9	148.0	127.9	130.9	135.7

[a]Chemical shifts are given in ppm (δ) measured at 100 MHz.
[b]Generated from reaction of TNA with 1 equiv PhO^-.
[c]CD_3CN-DME-d_{10} (1:1, v/v); obtained at –40°C.
[d]DMSO-d_6 at ambient temperature.
[e]Mesitoxyl *o*-Me δ 15.9; *p*-Me 20.2.

Combination of these observations with the kinetic preference shown by aryloxides for attack at the C-1 position of picryl alkyl ethers (6, 7) leads to assignment of the resonances at 8.62 and 7.17 to the ring protons of the C-1 PicOMes·$OMes^-$ adduct, **14** (Scheme 2). In this case, the H_3 and H_5 protons are non-equivalent as a result of steric interactions between the C-1 mesitoxy substituents and the flanking C-2,6 nitro groups. For example, if one of the C-2,6 NO_2 groups in **14** is twisted from the plane of the cyclohexadienate ring to relieve the proposed steric strain, then the negative charge of **14** could only be delocalized to the C-4 and one of the C-2,6 NO_2 groups. Thus, assuming that the C-4 and C-6 nitro groups form part of the conjugated anionic system, the C-2 nitro group and the moiety to which it is bonded would resemble an isolated nitroalkene, and H_3, in this example, would approximate a proton at the 2-position of a 1-nitroalkene (**14a**, Scheme 2). In this regard, it is noteworthy that the resonance for the olefinic proton at the 2-position of 1-nitrocyclohexene appears at 7.20 in DMSO-d_6 (21). Twisting of NO_2 groups out of the aromatic plane has been noted in numerous X-ray crystallographic studies of neutral nitroaromatic compounds that possess an alkoxy group adjacent to the nitro group (22).

As the temperature was gradually raised, the spectra obtained showed a sequential decline in the signals that represent **14** (Scheme 2). The spectrum acquired at –30°C (recorded ca. 30 min after the initial spectrum acquired at –40°C) lacked peaks of **14**; signals of **2** were notably broad. Upon further warming, peaks sharpened, and at –10°C the spectrum contained signals assigned to two C-3 $MesO^-$ adducts as follows: **12** at 8.44 (1H, d, J = 2.2, H_5) and 6.90 (1H, d, J = 2.2, H_3) and **13** at 8.44 (1H, d, J = 2.2, H_5 overlapped with H_5 of **12**) and 6.87 (1H, d, J = 2.2, H_3). Observation of signals of these Meisenheimer complexes in this system was in accord with their previous identification in the PicOPh–$MesO^-$ and PicOMes–PhO^- reactions and confirmed their assignment as adducts arising from attack of $MesO^-$ on PicOMes in all three studies.

At ambient temperature the peaks of **12** and **13** are replaced by those due to the C-3 PicOMes·OH^- adduct, **15** (Scheme 2). After monitoring the reaction for 12 h at room temperature, the singlet for **8** at 8.65 is also seen.

Discussion

Reaction pathways and classification of regioselectivity

The interactions of the series of O-nucleophiles, phenoxide (PhO^-), 2,4,6-trimethylphenoxide (mesitoxide, $MesO^-$), hydroxide (OH^-), and methoxide (MeO^-) ions with the picryl aryl ethers PicOPh, **1**, and PicOMes, **2**, provide interesting insights into the variable regioselectivity of Meisenheimer complex formation. On the basis of comparison of the pK_a values of the parent phenols (23) in water and with the assumption that nucleophilicity follows basicity (24), $MesO^-$ as the more basic aryloxide of the two would be expected to be a more reactive nucleophile than PhO^- (i.e., pK_a (PhOH) = 9.95; pK_a (MesOH) = 10.88, see also ref. 25). However, PhO^- may act as an ambident (C- and O-) nucleophile, whereas $MesO^-$ is restricted to O-attack. The *ortho*-Me groups in $MesO^-$ make it a sterically hindered nucleophile. This steric bulk would introduce further F-strain to attack at C-1, which would partly offset the higher nucleophilicity of $MesO^-$ compared with PhO^-. Therefore, the two aryloxides could display similar kinetic activity overall. Conversely, the steric factor may also render the resultant C-1 $MesO^-$ adduct significantly less stable than its C-1 PhO^- oxygen-centred counterpart. Consequently, these nucleophiles would show different thermodynamic preferences while displaying the same kinetic preference for C-1 attachment.

The ambident nature of PhO^- also results in the formation and observation of C-centred adducts as the final, stable Meisenheimer complexes observed in the reaction systems involving phenoxide as nucleophile. In each case, C-adducts were identified as the C-3 regioisomers bonded via the *para* site of phenoxide.

In all of the aryloxide systems examined, hydroxide adducts also formed during the period of study as a result of reaction with adventitious H_2O in the solvent systems. The assignments of these adducts was confirmed in separate control experiments that included reaction of **1** and **2** with tetramethylammonium hydroxide in DMSO and with potassium methoxide (in MeOH) in DMSO. As in other studies of picryl ether – alkoxide and picryl ether – hydroxide reactions (5), these localized O-nucleophiles reacted according to K3 classification in which attack at C-3 is kinetically pre-

ferred. On the other hand, the C-1 O-adducts **7** and (or) **10** (Scheme 1) and **16** and (or) **18** (Scheme 2) are not detected and represent metastable intermediates in the S_NAr displacement reaction to yield picrate (**8**), TNA, and phenol or mesitol.

The situation in the picryl aryl ether – methoxide systems is particularly informative. Although the C-1 adducts PicOPh·OMe^- (**10**) and PicOMes·OMe^- (**18**) are observed in the TNA–PhO^- (6*b*) and TNA–$MesO^-$ (6*c*) systems, respectively, these species are not observed in the present studies where the corresponding picryl aryl ethers react with methoxide to yield the C-3 adducts **9** and **17** as the only observable Meisenheimer complexes. It is important to note that in the TNA systems, **10** and **18** are the first and only adducts detected at –40°C in 1:1 MeCN–DME. Both adducts decompose to yield the C-3 hydroxide adduct of TNA via the thermodynamically unfavourable equilibrium between the aryloxide and adventitious water in the MeCN–DME medium (6*b*–6*d*, 9*a*). This observation suggests that the C-3 TNA·OH^- adduct is more stable than **10** and **18** and by extension the C-3 TNA·OMe^- adduct should also be more stable. These arguments suggest strongly that the inability to detect **10** and **18** in reactions of **1** and **2** with MeO^- stems from the fact that they are not as stable as the C-3 adducts **9** and **17**, respectively. The very slow rate of conversion of the C-3 PicOPh·OMe^- adduct **9** and C-3 PicOMes·OMe^- adduct **17** into the S_NAr products of TNA, PhO^-, $MesO^-$, and picrate (**8**) is consistent with this hypothesis. These arguments are summarized in the reaction coordinate diagram depicted in Fig. 2 for the reaction of PicOPh (**1**) with MeO^-. Here the C-1 O-adduct **10** is shown to be less stable than the C-3 adduct **9**. However, the S_NAr product from decomposition of **10** (TNA, PhO^-, and eventually picrate (**8**)) are the final products formed following irreversible processes. *Thus, even though the products from C-1 attack are thermodynamically favoured, the reactions of **1** and **2** with methoxide (and by extension hydroxide) can be designated as K3T3 on the basis of the kinetic and thermodynamic preferences in the initial reactions of **1** and **2** with the alkoxide (hydroxide) nucleophiles.*

Focusing on the aryloxide systems, PicOPh(**1**)–PhO^- and PicOMes(**2**)–$MesO^-$ are regarded as symmetrical systems, as the nucleophile and leaving group in the S_NAr process are the same; conversely, PicOPh(**1**)–$MesO^-$ and PicOMes(**2**)–PhO^- are regarded as nonsymmetric systems. In the symmetrical PicOPh(**1**)–PhO^- system, it is clear that reaction of PhO^- with **1** yields the C-1 PicOPh·OPh^- adduct, **3**, as the first observable phenoxide O-adduct (at –40°C). No C-3 phenoxide O-adduct (i.e., **4**, Scheme 1) is detected either prior to observation of **3** or later in the reaction. In our previous study of the TNA–PhO^- system we were able to demonstrate that a similar observation at low temperature indicated K1T1 regioselectivity (Fig. 1) in which formation of the corresponding C-1 TNA·OPh^- Meisenheimer complex was favoured by both kinetics and thermodynamics (6*b*). However, the TNA–PhO^- system had been previously examined by fast kinetic techniques that supported the assignment of the first formed O-adduct to the C-1 TNA·OPh^- species (8). Further, it had been established that the related TNB·OPh^- adduct could be identified and fully characterized by ^1H NMR spectroscopy under the same experimental conditions

Fig. 2. Qualitative reaction coordinate diagram for reaction of PicOPh (**1**) with MeO^-.

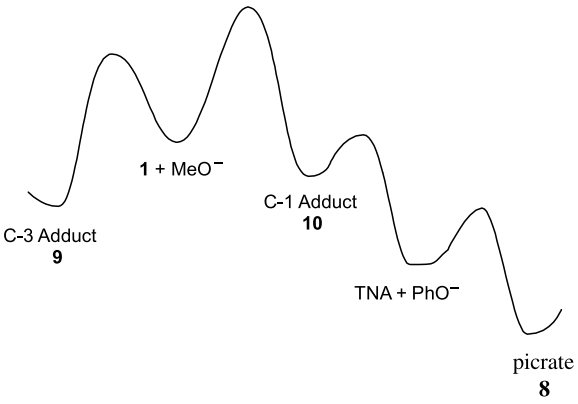

(9*a*). Since the TNB·OPh^- O-adduct is a reasonable model for a hypothetical C-3 TNA·OPh^- O-complex, it follows that any C-3 phenoxide O-adduct would have been observed if it had formed. It is, therefore, important in following this train of logic to note that the TNB·OPh^- adduct is also a structural analogue of the C-3 PicOPh·OPh^- Meisenheimer complex, **4**, and that **4** would be expected to be observed if it formed during the course of the reaction. *Thus, in the symmetrical PicOPh–PhO^- system, PhO^- (as an O-nucleophile) follows K1T1 regioselectivity.*

The next observable species, as a function of increasing temperature, is **6**, the C-3 PicOPh·OH^- complex. The necessary hydroxide is formed in low concentration via the thermodynamically unfavourable equilibrium between PhO^- and adventitious water in the MeCN–DME medium (6*b*–*d*, 9*a*). The timing of the appearance of the hydroxide adduct in these systems does not parallel the nucleophilicity of OH^- relative to PhO^- because of the expected significant difference in concentration of the two nucleophiles in these reaction systems. As the reaction proceeds, $PicO^-$ (picrate anion, **8**) and PhOH appear, presumably as decomposition products that arise from the transient C-1 PicOPh·OH^- adduct, **7** (Scheme 1), whose existence has been postulated in a number of related systems (6*b*–6*d*).

The ultimate product of thermodynamic control is the C-3 *para*-bonded C-adduct, **5**. Formation of this C-3 PicOPh·PhO(H)$^-$ Meisenheimer complex further illustrates the ambident (O- and C-) nucleophilic nature of phenoxide; compound **5** is formed with effective irreversibility. It is apparent that this C-3 C-adduct is the product of kinetic preference for C-attack at the 3-position. AM1 calculations (6*d*) suggest that the C-3 C-adduct is also the product of thermodynamic control. The thermodynamic preference for C-3 attack by carbon nucleophiles is also implicit in the reaction scheme of the VNS reaction (10). *Thus, in the PicOPh–PhO^- system, PhO^- (as a C-nucleophile) follows K3T3 regioselectivity.*

In the nonsymmetric systems (PicOPh(**1**)–$MesO^-$ and PicOMes(**2**)–PhO^-), reaction of **1** with $MesO^-$ forms the C-1 PicOPh·$OMes^-$ Meisenheimer complex, **11**, as the kinetically favoured species (Scheme 2). Although **11** is the dominant adduct observed in the first ^1H NMR spectrum acquired at –40°C, significant amounts of the C-1 PicOPh·OPh^- adduct, **3**, were also present. This observation im-

plied that **11** broke down to yield low concentrations of **2** and free PhO^-, which could then attack **1** to yield **3**. In this sense, two nucleophiles ($MesO^-$ and PhO^-) and two substrates (**1** and **2**) must be simultaneously present here and, by extension, in the other nonsymmetric PicOMes(**2**)–PhO^- reaction system.

Importantly, the initially formed C-1 O-adducts of **1** and **2** eventually give way to the C-3 mesitoxide O-centred adducts C-3 PicOMes·$OMes^-$, **12**, and the C-3 diadduct PicOMes·$(OMes)_2^{2-}$, **13**. The assignment of the structures of **12** and **13** as progeny of **2** was confirmed by the separate study of the symmetrical PicOMes(**2**)–$MesO^-$ system. Here, the initially formed C-1 PicOMes·$OMes^-$ adduct, **14**, decomposes in favour of the C-3 species, **12** and **13**. *Thus, the complexity of the nonsymmetric systems (PicOPh–$MesO^-$ and PicOMes–PhO^-) can render only a tentative classification as K1T3 (Fig. 1); however, as noted above, the simpler symmetrical PicOMes–$MesO^-$ system can be definitively classified as following K1T3 regioselectivity.*

Stereoelectronic stabilization of the C-1 adducts

Of the factors that stabilize the respective C-1 picryl ether O-adducts, stereoelectronic $n \rightarrow \sigma^*$ interactions have emerged from our analysis of the TNA–PhO^- and TNA–$MesO^-$ systems as an important mechanism of stabilization of these adducts (6*b–d*, 7). In brief, full $n \rightarrow \sigma^*$ stabilization is possible only when one O—R sigma bond is aligned antiperiplanar to one of the nonbonding lone pairs of the other C(1)-OR acetal-like group and vice versa (26), i.e., a "doubly antiperiplanar" conformation. We previously argued that in the C-1 TNA·OPh^- adduct (i.e., **10**), rotameric forms that would permit single $n \rightarrow \sigma^*$ interactions would be significantly populated in solution. Thus, as depicted in Fig. 3, Fig. 3*a*, which represents the most stable rotamer of **10**, will partake in this stereoelectronic stabilization through the antiperiplanar configuration of orbitals and consequently, adduct **10** is more stable than its C-3 counterpart (6*b*). However, from inspection of molecular models (Fieser or Darling) and on the basis of downfield ^{13}C chemical shifts (6*c*) that suggested puckering of the cyclohexadienate ring of the TNA^- moiety, it became apparent that the rotamer shown in Fig. 3*b* was preferred for the mesitoxide C-1 adduct of TNA, even though it does not permit stereoelectronic stabilization (6*c*, 7). Consequently, the C-1 TNA·$OMes^-$ adduct is not as stable as its C-3 analogue (6*c*).

A further factor impinges on the degree of $n \rightarrow \sigma^*$ stabilization provided to a given C-1 adduct that is geminally disubstituted by electronegative groups. Even if suitable doubly antiperiplanar conformers are readily accessible through rotation and even if such forms would be expected to be populated at a given temperature, the efficacy of the $n \rightarrow \sigma^*$ stabilization will depend on the relative energies of the two σ^* fragment orbitals. Thus, *n* donation from OPh in adduct **10** to the σ^* orbital of the OCH_3 fragment may be more or less effective than *n* donation from OCH_3 to the σ^* orbital of OPh. In general then, unsymmetrical C-1 adducts should exhibit less stereoelectronic stabilization than their symmetrical counterparts regardless of whether their most favourable rotameric forms are accessible or not (7, 26, 27). Consequently, the C-1 PicOPh·OMe^- adduct, **10**, the C-1 PicOMes·OMe^- adduct, **18**, the C-1 PicOMes·OPh^- adduct, **11**, and the C-1 hydroxide adducts, **7** and **16**, would all be expected to partake of less stereoelectronic stabilization than their symmetrical analogues. This factor, no doubt, partly accounts for the inability to observe the hydroxide adducts, for example.

Fig. 3. (*a*) Illustration of the stereoelectronic stabilization of the C-1 TNA·OPh^- adduct **10** through antiperiplanar interaction between the lone pair on the methoxy oxygen and the C—OPh bond; (*b*) Illustration of the TNA·$OMes^-$ adduct, where stereoelectronic stabilization as in (*a*) is not possible; (*c*) Illustration of the C-1 PicOPh·OPh^- adduct **3** where, as in (*a*), stereoelectronic stabilization is possible; (*d*) Illustration of the C-1 PicOMes·$OMes^-$ adduct **14** where, as in (*b*), stereoelectronic stabilization is not possible.

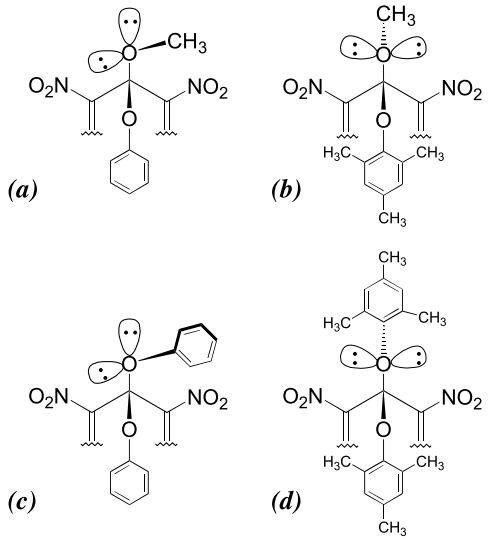

Focusing on the symmetrical aryloxide systems (PicOPh(**1**)–PhO^- and PicOMes(**2**)–$MesO^-$), whose regioselectivity could be clearly defined, it would be expected that the C-1 PicOPh·OPh^- adduct, **3**, if it could achieve suitable rotameric forms that would permit $n \rightarrow \sigma^*$ donation, would be stabilized relative to its C-3 counterpart, **4**. Therefore, the PicOPh–PhO^- system would be expected to display thermodynamic preference for formation of the C-1 adduct, i.e., T1 in the observed K1T1 regioselectivity, and **4** would not be detected. Relating the C-1 PicOPh·OPh^- adduct, **3**, to its TNA analogue (**10**, Fig. 3*a*), inspection of molecular models (Fieser or Darling) predicts that the rotamer represented in Fig. 3*c* would be the most stable for **3**. This configuration would be stabilized by $n \rightarrow \sigma^*$ donation, and consequently **3** would be more stable than its C-3 analogue **4**. These expectations are borne out by the observation of **3** as the sole O-adduct in this system.

For the PicOMes(**2**)–$MesO^-$ system, the rotamer represented in Fig. 3*d* is favoured for the C-1 PicOMes·$OMes^-$ adduct, **14**, on inspection of molecular models. This adduct is even more sterically congested than its TNA analogue (Fig. 3*b*), and **14** will be unable to derive any stabilization from $n \rightarrow \sigma^*$ donation. In fact, the non-equivalence of the 2,4,6-trinitrocyclohexadienate ring protons of **14** showed that to accommodate the bulky mesitoxyl groups at C-1, the adduct must sacrifice delocalization of negative charge into one of the *ortho* nitro groups as indicated in structure **14a**.

The C-1 PicOMes·OMes$^-$ adduct (**14**) has a relatively short lifetime even at low temperatures (i.e., **14** is no longer present in the spectrum taken at –30°C, a temperature at which the analogous C-1 PicOPh·OPh$^-$ adduct (**3**) is the only adduct seen in the PicOPh–PhO$^-$ system). *The lack of stereoelectronic stabilization and the consequent instability of 14 distinguishes the PicOMes–MesO$^-$ system that follows K1T3 regioselectivity from the PicOPh–PhO$^-$ system that exhibits K1T1 behaviour.*

Molecular orbital approaches to the kinetic preferences

Frontier molecular orbital analysis

An important question arises from the above considerations. If the PicOMes·OMes$^-$ adduct, **14**, is inherently so unstable, why does mesitoxide attack at C-1 occur at all? Moreover, given the steric bulk of the mesitoxide nucleophile, why is C-1 attack by MesO$^-$, particularly on the congested C-1 centre in PicOMes, **2**, favoured kinetically?

Molecular orbital theory, and, notably, the frontier molecular orbital (FMO) approach (28, 29), have been invoked to rationalize the regioselectivity in aromatic substitution reactions. As applied to the current systems, the FMO treatment holds that the preferred sites of attack will be those that permit maximum orbital overlap between the incoming (donor) nucleophile and the nitroaromatic (acceptor) substrate. In turn, this implies that the regioselectivity will be determined by the magnitude of the lowest unoccupied molecular orbital (LUMO) lobe at each ring carbon, as indicated by the orbital coefficients at each site, for a given nitroaromatic substrate.

Given the similarity in regioselectivity found for PicOPh, **1**, and PicOMes, **2**, in the current study and the behaviour of TNA with the same nucleophiles, namely PhO$^-$ (6*b*), MesO$^-$ (6*c*), and MeO$^-$ and OH$^-$ (6*b*, 6*c*, 5*a*, 5*b*), TNA would appear to be an acceptable general model for all picryl ethers. In this regard, we have undertaken AM1 calculations on TNA (and some related compounds (6*d*)). The two degenerate LUMOs of 1,3,5-trinitrobenzene become split upon introduction of the C-1 methoxyl group to form TNA. The AM1 calculated LUMO and superjacent unoccupied molecular orbital (SUMO) are illustrated in Fig. 4. The energy of the LUMO is –2.50 eV according to the AM1 calculation, while the SUMO is higher in energy at –2.39 eV (a difference of 0.11 eV or 2.5 kcal mol^{-1}).

Examination of the LUMO (Fig. 4) shows that C-1 is the site with the largest orbital coefficient. Interestingly, C-4, which bears a nitro group, is the site with the second highest orbital coefficient. The regioselectivity found should, in the FMO treatment, depend also on the energy of the highest occupied molecular orbital (HOMO) of the attacking nucleophile. The most favourable interaction will then be between nucleophile HOMO and substrate LUMO, when these are similar in energy.

Estimates of the HOMO energies of some of the anions have been made by Pearson (30) using the approximation that the electron affinity of the corresponding radicals (i.e., PhO$^\bullet$, OH$^\bullet$) represents the ionization potential (IP) of the anions that, according to Koopmans' theorem (31), is taken to be equal to the negative value of the HOMO energies. Therefore, the HOMO energy for PhO$^-$ and for OH$^-$ is estimated to be –2.35 and ca. –1.83 eV, respectively.

On the basis of the energetics, phenoxide (and, by extension, mesitoxide and other nucleophiles with relatively low-lying HOMO energies) may interact most strongly with the LUMO of TNA and, consequently, attack C-1, the site of highest orbital coefficient, preferentially. Conversely, hydroxide and methoxide may interact most strongly with the SUMO of TNA, which has its highest orbital coefficients at C-3 and C-5. Hence, aryloxides would show K1 behaviour while alkoxides and (or) hydroxide display K3 behaviour. However, such an analysis attributes significant changes in regioselectivity to relatively small energy differences; the energy gap between LUMO and SUMO is not large, and in fact, the HOMO of aryloxide nucleophiles would be expected to interact both with the LUMO and SUMO.

An alternative to the FMO approach is the configuration mixing model that is considered in the next section.

Configuration mixing model: Polar vs. SET pathways

The configuration mixing model advanced by Shaik, Pross, and Hoz in a series of articles (32) and reviews (16) defines the full reaction profile for an organic reaction by assuming, in general, that transition states possess varying proportions of covalent-bonding and radical character. This model provides a mechanistic spectrum between a single electron transfer (SET) pathway and a polar one, where the polar process involves synchronous electron shift and bond formation through a radical coupling pathway. In the SET route, SET precedes bond formation. Thus, which particular pathway is followed in any given reaction depends on the feasibility of coupling of the two spin-paired electrons (bond formation) following the electron shift. Factors governing SET vs. polar pathways include effects of donor–acceptor ability, steric interactions, the donor–acceptor bond strength, and radical delocalization (16*b*). Taking these factors into consideration allows assessment of which donor–acceptor pair is likely to follow the SET pathway.

In the present system, single electron transfer from the nucleophile to the picryl aryl ether would produce the radical anion of the picryl aryl ether and the requisite radical of the nucleophile. Change in nucleophile from an alkoxide-HO$^-$ to an aryloxide may cause a shift from a polar to a SET pathway. Electrochemical measurements in acetonitrile show that the one-electron half-peak oxidation potential ($E_{1/2}$) for the conversion of phenoxide into the phenoxyl radical is ~0.30 V vs. NHE. The corresponding value for HO$^-$ is ~0.6 V (33). The lower oxidation potential of phenoxide indicates that the phenoxyl radical is more stable than the hydroxyl radical as a consequence of the stabilizing effect exerted by the neighbouring aromatic ring on the radical centre. Further, since methyl substituents on a benzene ring are known to impart further stability to a benzylic (and presumably to an analogous aryloxide) radical, mesitoxyl radical would be expected to be more stable than phenoxyl radical and, therefore, to form even more readily (34, 35). Clearly the SET donor ability of the aryloxide is superior to that of alkoxides-HO$^-$. In terms of steric interactions, it is equally clear that mesitoxide is a more sterically hindered nucleophile than methoxide-HO$^-$. Steric hindrance favours the SET pathway since the polar pathway is energetically favourable when the reacting species can approach each other to within bonding distance. Steric repulsions will cancel en-

Fig. 4. Orbital coefficients (p_z), according to a semi-empirical calculation (AM1), for the lowest unoccupied molecular orbital (LUMO) and for the superjascent unoccupied molecular orbital (SUMO) of 2,4,6-trinitroanisole (TNA), a model for picryl ethers, generally. (The p_x and p_y coefficients are negligibly small). The LUMO, which is calculated to be lower in energy (–2.50 eV) than the SUMO (–2.39 eV), has its largest ring orbital coefficient at C-1 (i.e., –0.600), whereas the largest ring orbital coefficients in the SUMO are located at C-3 and C-5 (0.512 and –0.529, respectively).

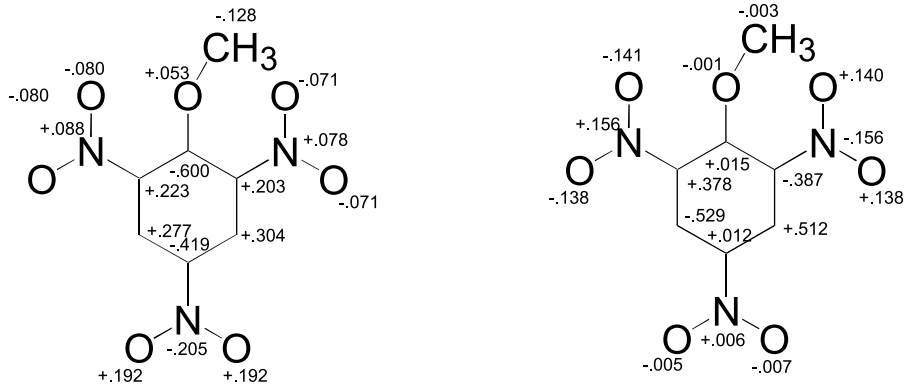

LUMO **SUMO**

ergy lowering because of bonding changes in the transition state, thus favouring the SET pathway, as SET processes take place at distances significantly greater than those at which incipient bonding takes place (16*b*). Furthermore, alkoxides and HO^- form strong bonds to give stable Meisenheimer complexes and generate localized radicals. These factors favour the polar pathway. In contrast, the aryloxides generate relatively unstable O-adducts that are transient in DMSO at room temperature (8, 9*a*) and delocalization of the aryloxide radical inhibits bond formation through radical coupling. These factors favour the SET pathway.

Shown in Fig. 5 is a schematic illustrating the relationship between the polar and SET reaction pathways (16*b*) for the present picryl aryl ether – nucleophile systems. The reactants are in the lower left corner where phenoxide and mesitoxide are represented as ArO^-. The polar process is indicated by the diagonal arrow, where both electron transfer and bond formation are synchronous.

The SET pathway depicted in Fig. 5 involves first electron transfer to generate the picryl aryl ether radical anion and the aryloxide radical ($ArO^{\cdot}$) shown in the upper left corner. The second step involves bond formation. Now the regioselectivity (C-1 or C-3) of Meisenheimer complex formation would be controlled by the spin density at the C-1 or C-3 positions of the radical anion of the picryl aryl ether, an intermediate on the reaction pathway. The position of higher spin density would be expected to be the site where radical coupling will be most favoured. Calculation of the spin density of the radical anion of TNA, the model for picryl ethers, using the AM1 method shows that C-1 is the site of highest spin density. Thus, subsequent radical combination to form the Meisenheimer complex would be expected to occur at C-1.

The configuration mixing model provides a rationale for the regioselectivity observed in reactions of picryl ethers with O-centred nucleophiles. The regioselectivity depends on the degree of concertedness of electron shift and bond formation. When electron shift and bond formation are concerted, C-3 attachment is kinetically favoured because of steric interactions at C-1. However, if the electron shift precedes bond formation, then the spin density of the picryl ether radical anion dictates C-1 attachment even though C-1 is clearly the more sterically hindered site.

In summary, on the basis of the above argument it can be concluded that *hydroxide and methoxide follow the polar (S_NAr) pathway; this will favour kinetically C-3 attachment due to F-strain at C-1. However, phenoxide and mesitoxide follow the SET pathway. In these cases, C-1 attachment is favoured kinetically due to the higher C-1 spin density in the radical anion of the picryl ether.*

Conclusions

The present results on the course of the reactions between picryl phenyl ether (PicOPh, **1**) and picryl mesityl ether (PicOMes, **2**) with the oxygen-nucleophiles, phenoxide, mesitoxide, hydroxide, and methoxide allow us to make the following conclusions.

The reactions of HO^- and MeO^- with **1** and **2** carried out in DMSO-d_6 at ambient temperature show K3 behaviour, as documented in numerous picryl ether – alkoxide systems (5*a–d*). In contrast, phenoxide and mesitoxide display kinetic preference for C-1 attachment, i.e., K1 behaviour. This observation is analogous to the reactivity of these aryloxide nucleophiles towards 2,4,6-trinitroanisole (6*b*, 6*c*), and now appears to be a general trend for the reactions of aryloxide nucleophiles with picryl ethers. For the reaction of phenoxide with **1**, the C-1 O-adduct is also thermodynamically favoured for phenoxide acting as an O-nucleophile. Stereoelectronic stabilization of the C-1 PicOPh·OPh^- adduct through $n \rightarrow \sigma^*$ donation confers thermodynamic preference on this C-1 adduct relative to its C-3 oxygen-centred regioisomer. With mesitoxide ion, the C-1 adducts of both substrates are less stable than their C-3 counterparts. In these cases the steric congestion in the C-1 adducts associated with the presence of the *ortho* methyl groups of mesitoxyl moiety precludes significant stereoelectronic stabilization. Now the C-3 adducts of mesitoxide are more stable and the

Fig. 5. Schematic of a potential energy surface diagram illustrating the relationship between polar and SET reaction pathways for reaction of **1** and (or) **2** with aryoxide (ArO^-) nucleophiles to give the C-1 Meisenheimer adducts.

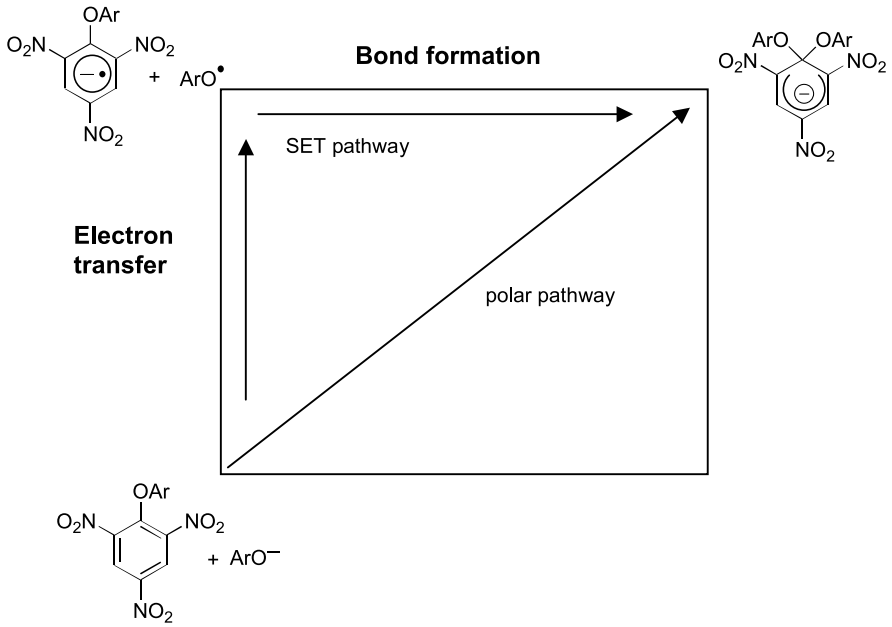

initially formed C-1 adducts decline in favour of their C-3 regioisomers.

Although steric inhibition of stereoelectronic stabilization can account for the changeover in adduct stability (i.e., C-1 PhO^- adduct of **1** are more stable than its C-3 counterpart, whereas the C-1 $MesO^-$ adducts of **1** and **2** are less stable than their C-3 isomers), there is still kinetic preference to formation of the C-1 adducts of **1** and **2** even when the attacking nucleophile is the bulky mesitoxide ion. Frontier molecular orbital considerations suggest that all nucleophiles would preferentially attack the C-1 site of picryl ethers, based on AM1 calculations of 2,4,6-trinitroanisole (TNA), as a general model for picryl ethers. An alternative explanation, which we propose, is that the reactions involving the aryloxides do not follow the polar S_NAr pathway, but rather proceed according to the SET pathway outlined in Fig 5.

Experimental

Materials and methods

2,4,6-Trinitrophenyl phenyl ether (PicOPh,**1**) was prepared from picryl chloride and potassium phenoxide in ethanol as described by Dyall (36), mp 154–155°C (lit. (36) value mp 153–154°C). 2,4,6-Trinitrophenyl-2′,4′,6′-trimethylphenyl ether (PicOMes, **2**) was prepared from picryl chloride and ethanolic potassium mesitoxide, mp. 157–158°C (lit. (37) value mp 154–155°C). Picryl chloride used in these preparations resulted from the reaction of pyridinium picrate with $POCl_3$ (38), mp. 80–81°C, after recrystallization from CCl_4 (lit. (39) value mp 81°C). Acetonitrile-d_3 and dimethoxyethane-d_{10} (Merck) were dried by sequential treatment with 4 Å molecular sieves as advocated by Burfield et al. (17). 1,4-Dibromobenzene (DBB; Eastman) was recrystallized from ethanol and dried in vacuo prior to use as an internal integration standard in the NMR experiments. Potassium phenoxide and mesitoxide were prepared from the respective phenol and standard MeOK–MeOH in an N_2-filled glovebox as described previously (6*b*, 6*c*). 2,4,6-Trimethylphenol (mesitol; Aldrich) was recrystallized from petroleum ether and dried in vacuo before use. Trifluoroacetic acid (TFA; Aldrich) and tetramethylammonium hydroxide (Me_4NOH, 25 wt % solution in water; Aldrich) were used without further purification. Melting points were measured on a Thomas Hoover capillary apparatus and are not corrected.

NMR experiments: General

NMR experiments were carried out using a Bruker AM-400 specrometer (^1H: 400.1 MHz, ^{13}C: 100.0 MHz) in MeCN-d_3:DME-d_{10} (1:1 v/v) or in dried DMSO-d_6. In the mixed solvent system, CD_2HCN served as chemical shift reference (^1H: δ = 1.93 ppm) and lock signal, whereas resonances found in spectra determined in DMSO were referenced to the peak for residual CD_3SOCD_2-H in the solvent (^1H: δ = 2.50 ppm). Chemical shifts are given in parts per million (ppm) and coupling constants (*J*) are reported in hertz. Wilmad PP-507 NMR tubes (5 mm) were used in all experiments. All stock solutions were prepared in the appropriate solvents under a nitrogen atmosphere. NMR tubes were capped with rubber septa and swept out with dry N_2 prior to injection of the reactants into the NMR tube with a gas-tight syringe.

Low temperature NMR experiments in MeCN–DME (1:1)

Typically, a weighed quantity of the aryloxide was dissolved in a 1:1 (v/v) mixture of MeCN-d_3:DME-d_{10} under a nitrogen atmosphere such that 300 μL of this stock solution would yield 1–1.5 equiv of the aryloxide relative to the substrate. An aliquot of the stock solution (300 μL) was injected into the NMR tube, and the solution frozen by immersion in liquid N_2. To the frozen solution, 1 equiv of PicOPh or

PicOMes was injected by a gas-tight syringe (200 μL; final concentrations 0.06–0.09 M). The final mixture was placed in a dry ice – acetone bath that had been maintained at –50°C. The contents of the tube were allowed to mingle at this temperature. The tube was inverted several times to promote mixing and was then immersed again in liquid N_2. The tube was transferred to the spectrometer probe (at –40°C), the instrument was tuned as previously described (6*b*), and spectra were recorded at various intervals. A standard collection of FID would be made at 3, 5, 7, and 9 min and then as warranted by observed changes in the spectrum. Simultaneously, the temperature of the probe was gradually raised.

Room temperature experiments in DMSO

A solution of the substrate was prepared in DMSO-d_6 under an N_2 atmosphere. An aliquot of this solution was transferred via syringe into an NMR tube and an initial spectrum run to ascertain the purity of the substrate. To this solution 1 equiv of nucleophile was injected through the septum and spectra were recorded as rapidly as possible initially and then at longer times as the reaction proceeded. 1,4-Dibromobenzene was present in the solution of the substrate and in the NMR tube as an internal integration standard.

Molecular orbital calculations

Semi-empirical calculations were performed using AMPAC version 2.10 of AM1 (15*a*) on an IBM 3081 computer. The structure of 2,4,6-trinitroanisole (TNA) was calculated using the PRECISE option within the restricted Hartree–Fock (RHF; closed shell) scheme. The TNA structure was fully optimized following a Fletcher–Powell minimization (40) to a self-consistent field (SCF) that satisfied Herbert's test. The final structure was characterized as a local minimum when no negative force constants were obtained using the FORCE option.

Acknowledgments

This research has been financed by a number of agencies. The support of the Natural Sciences and Engineering Research Council of Canada (NSERC) (to E.B.) and Wake Forest University (to R.A.M.) as well as the award of an R.T. Mohan Fellowship (to R.M.T.) is gratefully acknowledged. Discussions with Professors S. Hoz and F. Terrier were helpful, as always, and are appreciated.

References

1. (*a*) R.A. Foster. J. Phys. Chem. **84**, 2135 (1980); (*b*) M.A. Slifkin. Mol. Interact. **2**, 271 (1981).
2. (*a*) R. Bacaloglu, C.A. Bunton, and G. Cerichelli. J. Am. Chem. Soc. **109**, 621(1987); (*b*) R. Bacaloglu, C.A. Bunton, G. Cerichelli, and F. Ortega. J. Am. Chem. Soc. **110**, 3495 (1988); (*c*) R. Bacaloglu, C.A. Bunton, and F. Ortega. Int. J. Chem. Kinet. **20**, 195 (1988); (*d*) R. Bacaloglu, A. Blasko, C.A. Bunton, F. Ortega, and C.Zucco. *In* Atual. Fis-Quim. Org. Conf. Latinoam. Fis-Quim. Org. 1st, *Edited by* E. Humeres. 1991. p. 165; (*e*) R. Bacaloglu, A. Blasko, C.A. Bunton, E. Dorwin, F. Ortega, and C. Zucco. J. Am. Chem. Soc. **113**, 238 (1991); *(f)* R. Bacaloglu, A. Blasko, C.A. Bunton, F. Ortega, and C. Zucco. J. Am. Chem. Soc. **114**, 7708 (1992).
3. (*a*) E.A. Symons and E. Buncel. Can. J. Chem. **50**, 1729 (1972); (*b*) E. Buncel and E.A. Symons. J. Org. Chem. **38**, 1201 (1973); (*c*) E. Buncel and A.W. Zabel. Can. J. Chem. **59**, 3168; 3177 (1981).
4. (*a*) E. Buncel, J.M. Dust, K.T. Park, R.A. Renfrow, and M.J. Strauss. *In* Nucleophilicity. *Edited by* J.M. Harris and S.P. McManus. ACS Adv. in Chem. Ser. 215. American Chemical Society, Washington, D.C. 1987. pp 369–383; (*b*) E. Buncel, M.R. Crampton, M.J. Strauss, and F. Terrier. Electron deficient aromatic – and heteroaromatic – base interactions. The chemistry of anionic sigma complexes. Elsevier, Amsterdam. 1984; (*c*) E. Buncel. *In* The chemistry of functional groups. Supplement F. The chemistry of amino, nitro, and nitroso compounds. *Edited by* S. Patai. Wiley, London. 1982; (*d*) F. Terrier. Chem. Rev. **82**, 77 (1982); (*e*) F.A. Artamkina, M.P. Egorov, and I.P. Beletskaya. Chem. Rev. **82**, 427 (1982); (*f*) C.F. Bernasconi. MTP Int. Rev. Sci. Org. Chem. Ser. One, **3**, 33 (1973); (*g*) M.J. Strauss. Chem. Rev. **70**, 667 (1970); (*h*) E. Buncel, A.R. Norris, and K.E. Russell. Quart. Rev. Chem. Soc. London, **22**, 123 (1968).
5. (*a*) K.L. Servis. J. Am. Chem. Soc. **87**, 5495 (1965); (*b*) K.L. Servis. J. Am. Chem. Soc. **89**, 1508 (1967); (*c*) R.A. Foster, C.A. Fyfe, P.H. Emslie, and M.I. Foreman. Tetrahedron, **23**, 227 (1967); (*d*) C.F. Bernasconi. J. Am. Chem. Soc. **92**, 4682 (1970); (*e*) G. Baldini, G. Doddi, G. Illuminati, and F. Stegel. J. Org. Chem. **41**, 2153 (1976); (*f*) M.P. Simonnin, M.J. Pouet, and F. Terrier. J. Org. Chem. **43**, 855 (1978); (*g*) A.D.A. Alaruri and M.R. Crampton. J. Chem. Res. Synop. 140 (1980); J. Chem. Res. Miniprint, 2157 (1980); (*h*) M.P. Simonnin, J.C. Halle, F. Terrier, and M.J. Pouet. Can. J. Chem. **63**, 866 (1985).
6. (*a*) E. Buncel, S.K. Murarka, and A.R. Norris. Can. J. Chem. **62**, 534 (1984); (*b*) E. Buncel, J.M. Dust, A. Jonczyk, R.A. Manderville, and I. Onyido. J. Am. Chem. Soc. **114**, 5610 (1992); (*c*) R.A. Manderville and E. Buncel. J. Am. Chem. Soc. **115**, 8985 (1993); (*d*) E. Buncel, R.M. Tarkka, and J.M. Dust. Can. J. Chem. **72**, 1709 (1994).
7. E. Buncel, J.M. Dust, and F. Terrier. Chem. Rev. **95**, 2261 (1995).
8. C.F. Bernasconi and M.C. Muller. J. Am. Chem. Soc. **100**, 5530 (1978).
9. (*a*) E. Buncel and R.A. Manderville. J. Phys. Org. Chem. **6**, 71 (1993); (*b*) E. Buncel and J.M. Dust. Can. J. Chem. **66**, 1712 (1988); (*c*) E. Buncel and W. Eggimann. J. Am. Chem. Soc. **99**, 5958 (1977); (*d*) E. Buncel, J.G.K. Webb, and J.F. Wiltshire. J. Am. Chem. Soc. **99**, 4429 (1977); (*e*) E. Buncel and W. Eggimann. Can. J. Chem. **54**, 2436 (1976); (*f*) E. Buncel, A. Jonczyk, and J.G.K. Webb. Can. J. Chem. **53**, 3761 (1975); (*g*) E. Buncel and J.G.K. Webb. J. Am. Chem. Soc. **95**, 328 (1973).
10. (*a*) M. Makosza. Pol. J. Chem. **66**, 3 (1992); (*b*) M. Makosza,W. Daniekiewicz, and E. Wojciechowski. Phosphorus Sulfur Silicon Relat. Elem. **53**, 457 (1990); (*c*) M. Makosza and A. Kinowski. Bull. Pol. Acad. Sci. **37**, 127 (1989); (*d*) M. Makosza. Russ. Chem. Rev. **58**, 747 (1989); (*e*) M. Makosza and J. Winiarski. Acc. Chem. Res. **20**, 282 (1987).
11. (*a*) M.R. Crampton and V. Gold. J. Chem. Soc. 4293 (1964); (*b*) M.R. Crampton and V. Gold. J. Chem. Soc. B, 893 (1966).
12. (*a*) C.F. Bernasconi. J. Am. Chem. Soc. **93**, 6975 (1971); (*b*) M.R. Crampton and H.A. Khan. J. Chem. Soc. Perkin Trans. 2, 1173 (1972); (*c*) M.R. Crampton, B. Gibson, and F.W. Gilmore. J. Chem. Soc. Perkin Trans. 2, 91 (1979); (*d*) R. Destro, C. Grammicioli, and M. Simonetta. Acta Crystallogr. Sect. B Struct. Crystallogr. Cryst. Chem. **24**, 1369 (1968);

(*e*) H. Ueda, N. Sakabe, J. Tanaka, and A. Furusaki. Bull. Chem. Soc. Jpn, **41**, 2866 (1968).
13. M.R. Crampton. Adv. Phys. Org. Chem. **7**, 211 (1969).
14. A. Cooney and M.R. Crampton. J. Chem. Soc. Perkin Trans. 2, 1973 (1984).
15. (*a*) M.J.S. Dewar, E.G. Zoeblisch, E.F. Healy, and J.J.P. Stewart. J. Am. Chem. Soc. **107**, 3902 (1985); (*b*) M.J.S. Dewar and K.M. Dieter. J. Am. Chem. Soc. **108**, 8075 (1986).
16. (*a*) A. Pross and S.S. Shaik. Acc. Chem. Res. **16**, 363 (1983); (*b*) A. Pross. Acc. Chem. Res. **18**, 212 (1985); (*c*) S. Hoz. Acc. Chem. Res. **26**, 69 (1993).
17. D.R. Burfield and R.H. Smithers. J. Org. Chem. **43**, 3966 (1978).
18. (*a*) B. Gibson and M.R. Crampton. J. Chem. Soc. Perkin Trans. 2, 648, (1979); (*b*) C.F. Bernasconi, J. Fassberg, R.B. Killiom, Jr., D.F. Schuck, and Z. Rappoport. J. Am. Chem. Soc. **113**, 4937 (1991).
19. (*a*) J.F. Bunnett and R.E. Zahler. Chem. Rev. **49**, 273 (1951); (*b*) J.F. Bunnett. Quart. Rev. Chem. Soc. London, **12**, 1 (1958); (*c*) J.A. Orvik and J.F. Bunnett. J. Am. Chem. Soc. **92**, 2417 (1970).
20. (*a*) J. Miller. Nucleophilic aromatic substitution. Elsevier, Amsterdam. 1968; (*b*) F. Terrier. Nucleophilic aromatic displacement. The influence of the nitro group. VCH, New York. 1991.
21. C.J. Pouchert. The Aldrich library of NMR spectra. Vol. 1. Aldrich, Milwaukee, WI. 1986. p. 355
22. (*a*) J. Trotter. Acta Crystallogr. **12**, 605 (1959); (*b*) P. Coppens. Acta Crystallogr. **17**, 573 (1964); (*c*) F. Terrier, L. Xaio, P.G. Farrell, and D. Moskowitz. J. Chem. Soc. Perkin Trans. 2, 1259 (1992); and refs. cited therein.
23. G.R. Sprengling and C.W. Lewis. J. Am. Chem. Soc. **75**, 5709 (1953).
24. F. Bordwell, T.A. Cripe, and D.L. Hughes. *In* Nucleophilicity. *Edited by* J.M. Harris and S.P. McManus. Adv. Chem. Ser. **215**. American Chemical Society, Washington, D.C. 1987. pp 137–155.
25. (*a*) E.H. Baughman and M.M. Krevoy. J. Phys. Chem. **4**, 421 (1974); (*b*) F.G. Bordwell. Acc. Chem. Res. **21**, 456 (1988).
26. (*a*) A. J. Kirby. The anomeric effect and related stereoelectronic effects at oxygen. Springer-Verlag, Berlin. 1983. pp 9–11, 82, 90, 135–136; (*b*) P. Deslongchamps. Stereoelectronic effects in organic chemistry. Pergamon Press, New York. 1983. pp 5–20.
27. M.L. Sinnott. Adv. Phys. Org. Chem. **24**, 114 (1988).
28. K. Fukui, T. Yonezawa, C. Nagata, and H. Shingu. J. Chem. Phys. **22**, 1433 (1954).
29. I. Fleming. Frontier orbitals and organic reactions. Wiley. New York. 1976.
30. R.G. Pearson. Inorg. Chem. **27**, 734 (1988).
31. T. Koopmans. Physica Utrecht, **1**, 34 (1934).
32. (*a*) S.S. Shaik. Prog. Phys. Org. Chem. **15**, 197 (1985); (*b*) S.S. Shaik. J. Am. Chem. Soc. **103**, 3692 (1981); (*c*) A. Pross. Isr. J. Chem. **26**, 360 (1985).
33. P.K.S. Tsang, P. Cofre, and D.T. Sawyer. Inorg. Chem. **26**, 3604 (1987).
34. (*a*) J.M. Dust and D.R. Arnold. J. Am. Chem. Soc. **105**, 1221 (1983); (*b*) D.D.M. Wayner and D.R. Arnold. Can. J. Chem. **62**, 1164 (1984).
35. R.A. Jackson and M. Sharifi. J. Chem. Soc. Perkin Trans. 2, 775 (1996).
36. L.K. Dyall. J. Chem. Soc. 5160 (1960).
37. L.B. Clapp, H. Lacey, G.G. Beckwith, R.M. Srivastava, and N. Muhammad. J. Org. Chem. **33**, 4262 (1968).
38. R. Boyer, E.Y. Spencer, and G.F. Wright. Can. J. Res. **24B**, 200 (1946).
39. P.F. Frankland and F.H. Garner. Chem. Ind. London, **39**, 257 (1921).
40. R. Fletcher and M.J.D. Powell. Comput. J. **6**, 163 (1963).